Journal of Applied Polymer Science

Thermal, Crystallization, and Dynamic Rheological Behavior of Wood Particle/HDPE Composites: Effect of Removal of Wood Cell Wall Composition

Rongxian Ou,[1,2] Yanjun Xie,[1] Qingwen Wang,[1] Shujuan Sui,[1] Michael P. Wolcott[2]

[1]Key Laboratory of Bio-Based Material Science and Technology (Ministry of Education), Northeast Forestry University, Harbin 150040, China

[2]Composite Materials and Engineering Center, Washington State University, Pullman, Washington 99164

Correspondence to: Q. Wang (E-mail: qwwang@nefu.edu.cn) or M.P. Wolcott (E-mail: wolcott@wsu.edu)

ABSTRACT: This study investigated the effect of removal of wood cell wall composition on thermal, crystallization, and dynamic rheological behavior of the resulting high density polyethylene (HDPE) composites. Four types of wood particle (WP) with different compositions: native wood flour (WF), hemicellulose-removed wood particle (HR), lignin-removed wood particle (holocellulose, HC), and both hemicellulose and lignin removed particle (α-cellulose, αC) were prepared and compounded with HDPE using extruder, both with and without maleated polyethylene (MAPE). Results show that removal of the hemicellulose improved the thermal stability of composites, while removal of the lignin facilitated thermal decomposition. WPs acted as nucleating agents and facilitated the process of crystallization, thereby increasing the crystallization temperature and degree of crystallinity. The crystallization nucleation and growth rate of αC and HR based composites without MAPE decreased, as compared with WF based one. Composite melts with and without MAPE exhibited a decreasing order of storage modulus, loss modulus, and complex viscosity as αC > WF > HR > HC and αC > HR > WF > HC, respectively. © 2014 Wiley Periodicals, Inc. J. Appl. Polym. Sci. **2014**, *131*, 40331.

KEYWORDS: composites; crystallization; rheology; thermal properties

Received 28 October 2013; accepted 18 December 2013
DOI: 10.1002/app.40331

INTRODUCTION

Recently, wood plastic composites (WPCs) have attained prevalent use in building materials, automobile components, and infrastructure.[1] In general, large amounts of wood are preferred to achieve good appearance and performance, low costs, and increased environmentally friendliness. However, high wood content leads to a considerable increase of melt viscosity, which can cause miscellaneous processing difficulties such as flow instabilities, surface defects, and even failure of extrusion melt.[2–4] These difficulties result from incorporation of rigid cell wall structure.[5] Increasing the thermoplasticity of wood cell walls may be a strategy to improve the processibility of WPCs.

Cellulose, hemicellulose, and lignin are three major components of lignocellulosics in varying amounts according to plant type (hardwood, softwood, agricultural residues, and energy crops).[6] Cellulose microfibrils with high crystallinity are coated and tethered by hemicelluloses, which are embedded within a three-dimensional matrix of lignin.[7] Properties of WPCs can depend on the intrinsic properties and structure of the lignocellulosic fibers used, as well as cell wall components and microstructure. The absence of hemicellulose or lignin has been shown to influence the properties of the lignocellulosic fibers and therefore the end-use performance of the composites.[8–11]

Andrusyk et al.[12] showed that hot-water hemicellulose extraction causes an increase in compatibility between wood and polypropylene (PP), while mechanical properties are not adversely affected. Hosseinaei et al.[9,13] investigated injection-molded PP composites filled with hemicellulose-extracted Southern Yellow Pine through liquid hot-water treatment (extraction at 140, 155, and 170°C for 60 min). They found decreased water absorption, increased tensile properties, and improved mold resistance in the resulting composites, which was attributed to the decreased hygroscopicity of the extracted wood. Pelaez-Samaniego et al.[14] used hot water extracted ponderosa pine with bark intact to make high density polyethylene (HDPE) and PP composites. The mechanical properties were either unchanged or improved, and the water absorption decreased.

Karimi et al.[15] investigated hot-pressed PP composites filled with delignified hornbeam fiber by a Kraft pulping process at

170°C. They showed that delignification improved the tensile strength, tensile modulus, and water resistance of the resulting composites. Fabiyi et al. produced HDPE[11] and polyvinyl chloride[16] composites from pine, extractives-free pine, and pine holocellulose (HC; delignified) and found that HC-based composites had the lowest changes in total color and lightness for both outside and xenon-arc weathering.

Our previous research[17] has revealed that the removal of hemicellulose by alkaline treatment can significantly increase the dimensional stability of the HDPE composites, and improve the tensile strength, toughness, and impact strength. Removal of lignin by acid-chlorite delignification can increase the tensile modulus, while decreasing the dimensional stability of the composites. Removing both hemicellulose and lignin resulted in the highest values for tensile strength, elongation at brake, toughness, and impact strength for composites.

The changes in chemical composition and microstructure of cell wall caused by removing hemicellulose and/or lignin may influence the plastic deformability of cell wall and, accordingly, the processibility of WPCs. Therefore, this study aims to elucidate the effect of removal of specific cell wall composition (hemicellulose and/or lignin) on the thermal stability, crystallization behavior, and dynamical rheological properties of the resulting HDPE composites.

EXPERIMENTAL

Materials

Hybrid poplar (*Populus ussuriensis* Kom.), which is fast growing, low cost, and highly abundant in China, was used in this study. Wood flour was prepared from sapwood chips in a hammer mill to pass through 80 PVC 100 mesh sieves. HDPE pellets (5000S) purchased from Daqing Petrochemical, China, bear a density of 0.954 g cm^{-3} and a melt flow index of 0.7 g/10 min (190°C, 2.16 kg according to ASTM D1238). The HDPE pellets were chilled and ground to a fine powder for subsequent use. Maleated polyethylene (MAPE, A-C® 575A) was supplied by Honeywell International, whit a MA grafting ratio of 3 wt % and a saponification value of 35 mg KOH/g.

Preparation of Wood Particles (WPs)

Four types of WPs were prepared from the 80–100 mesh poplar flour, following methods reported in the previous literature:

1. WF - Extracted wood flour: Wood flour was extracted in a Soxhlet extractor with a mixture of ethanol and toluene (1 : 2 in volume) for 6 h to remove soluble extractives.
2. HR - Hemicellulose-removed WF: Hemicelluloses were removed from the WF according to TAPPI 203,[18] leaving lignin and cellulose.
3. HC - Holocellulose (delignified WF): The WF was delignified using a NaClO2 treatment, leaving hemicelluloses and cellulose.[19]
4. αC - α-Cellulose (both hemicellulose and lignin removed WF): The HC was further treated with a 17.5% NaOH aqueous solution to remove hemicelluloses according to TAPPI 203.18

These chemical treatments can potentially alter the size of WPs. To remove the confounding variable of particle size, all particles were pulverized to 100–160 mesh using an herb grinder with knife. These particles were dried at 105°C for 24 h, and then stored in a sealed container for use.

Preparation of Composite Specimens

WPs were dry-mixed with the HDPE powder and MAPE at a specific ratio as shown in Table I. They were compounded using a corotating twin-screw extruder (diameter = 8 mm and L/D = 40) equipped with a volumetric feeder and a strand pelletizer (Leistritz ZSE-18, Leistritz Extrusionstechnik GmbH, Germany). The extrusion temperature ranging from 150 to 175°C was individually controlled in eight temperature zones along the extruder barrel. The extrudate was cut into pellets using the strand pelletizer. The pellets were then injection-molded (SE50D, Sumitomo Heavy Industries, Japan) into standard specimens for mechanical testing. Injection and mold temperatures were 180 and 50°C, respectively.

Characterization

Morphological Analysis. Sections of the impact test specimens were cryo-microtomed (RMC CR-X cryo-ultramicrotome) perpendicular to the injection flow direction at −120°C using a glass knife. The sectioned surfaces were subsequently dried, sputter-coated with gold, and then observed with a field emission scanning electron microscope (FE-SEM, Quanta 200F, FEI Company) at an accelerated voltage of 30 kV.

Thermogravimetric Analysis (TGA). TGA was performed on a thermal analyzer (SDT Q600, TA Instruments, New Castle) under N_2 atmosphere with a purge gas flow of 100 mL min^{-1}.

Table I. Formulations of the Composites

Sample	Particle type	Particle (wt %)	HDPE (wt %)	MAPE (wt %)
WF/PE	WF	40	60	0
HR/PE	HR	40	60	0
HC/PE	HC	40	60	0
αC/PE	αC	40	60	0
WF/PE/MA	WF	40	58	2
HR/PE/MA	HR	40	58	2
HC/PE/MA	HC	40	58	2
αC/PE/MA	αC	40	58	2

Powdered samples (6–8 mg) were heated from room temperature to 650°C at a heating rate of 10°C min^{-1}. Three replicates were used for each formulation.

Differential Scanning Calorimetry (DSC) Analysis. Melting and crystallization behaviors of the composites were measured using a heat flux DSC (DSC 822e, Mettler Toledo) under N_2 flow (80 mL min^{-1}) cooling with liquid nitrogen. Temperature and enthalpy calibrations were steadily conducted using high purity indium and zinc standards. Samples of ~6 mg were placed in 40 μL aluminum crucible and heated from 25 to 170°C at 30°C min^{-1}, hold at 170°C for 5 min to erase any thermal history. Then samples were cooled down to 25°C at 10°C min^{-1} and heated again to 170°C at 10°C min^{-1}. The degree of crystallinity (X_c, %) was determined from the second melting enthalpy values using the following equation:

$$X_c(\%) = \frac{\Delta H_f}{W \Delta H_f^0} \times 100 \quad (1)$$

where ΔH_f and ΔH_f^0 are the enthalpy of fusion of the measured sample and 100% crystalline HDPE ($\Delta H_f^0 = 290\,J\,g^{-1}$),[20] respectively, and W is the weight fraction of HDPE in the composites. Three replicates were used for each formulation.

Dynamic Rheological Tests. Dynamic rheological tests were conducted using a rotational rheometer (Discovery HR-2, TA Instruments, New Castle) equipped with a pair of parallel plates (2 mm distance between plates and 25 mm in diameter). The extruded pellets of WP/HDPE compound prepared at Section "Preparation of Wood Particles" were injection-molded into test samples measuring 25 mm (diameter) × 2.2 mm (thickness) using a mini injection molder (Haake MiniJet, Thermo Scientific, Germany). The zone and mold temperatures were maintained at 180 and 50°C, respectively. Prior to testing, the molten sample was equilibrated for 5 min in the testing chamber to erase any previous thermal and deformation history. Isothermal dynamic frequency sweep (0.1–628.3 rad s^{-1}) experiments were performed at a given strain amplitude of 0.05% in linear region at 175°C. Three replicates were used for each formulation.

RESULTS AND DISCUSSION

Morphological Analysis

Interfacial delamination can be clearly identified on the sectioned surfaces of the composites without MAPE [Figure 1(a,c,e,g)]. When the samples were cooled to −120°C during sample preparation, the gap between the particles and the HDPE matrix could be increased, resulting from their difference in expansion coefficient and poor interfacial adhesion. Removal of hemicelluloses caused fewer interfacial separations compared with the other composites without MAPE [Figure 1(c)]. This may be due to increased hydrophobicity of HR from the removal of hydrophilic hemicelluloses. This promotes the wettability by the HDPE matrix.[9] Removal of lignin seemed to facilitate the interfacial separation [Figure 1(e)]. The cell structure was nearly indiscernible in the αC, resulting from both the delignification and hemicellulose removal, which also exhibited a much smaller diameter than that of WF [Figure 1(g,h)].

The interfacial adhesion between the WP surface and HDPE was improved by adding 2% MAPE, while in the inner part of WP, the interfacial adhesion was still poor, as indicated by the gap between the cell wall and the HDPE [Figure 1(b,d)]. This may be because the MAPE mainly reacted with the —OH groups on the WP surface. The strong interfacial interaction on the particle surface can withstand the stress caused by the shrinkage of HDPE matrix at −120°C, while the inner parts of the WP were laniated by the shrinkage stress.

The cell walls of WF [Figure 1(a,b)] and HR [Figure 1(c,d)] remained intact in the composites with and without MAPE during processing, and exhibited less compression of collapse than HC. Likewise, the lumens of these particles were filled with the HDPE matrix (darker-colored phase), which moved into these void structures under pressure during extrusion and/or injection processing. In contrast, the cell walls of HC particle [Figure 1(e,f)] were highly compressed (as indicated by arrows) and little HDPE was observed to fill in the bundles of HC particle. Interpretation of this morphology suggests that the HC particles exhibit enhanced flexibility and deformability compared with WF and HR particles containing lignin.

Thermogravimetric Analysis

It is assumed that the moisture absorbed by WP can be completely removed at 150°C. The composite weight at 150°C is thus considered as the initial weight and the onset decomposition temperature (T_{on}) is defined at 1% weight loss based on the initial weight. Decomposition of neat HDPE started at around 430°C, and nearly 100% decomposition occurred at 500°C [Figure 2(a)]. This result was confirmed by the presence of a single peak ($T_{p,h}$, maximum rate of decomposition) in the derivative thermogravimetric curve (DTG) at 478°C (Table II). The particle size of WF should have no significant influence on the TGA results. The DTG curve of WP showed two decomposition steps [Figure 2(a)]. The first decomposition shoulder in the range of 220–300°C indicated the decomposition of hemicellulose, parts of lignin, and amorphous cellulose. The second peak assigned to the cleavage of glycosidic linkage of cellulose was observed in the temperature range from 300 to 400°C.[21] Aromatic ether linkages in lignin are more stable to thermal degradation than hemicellulose and cellulose.[22] The decomposition of lignin usually can run through the entire temperature range and overlap with the peaks of hemicelluloses and cellulose.

The DTG peak of HR at 220–300°C was obscured, resulting from absence of hemicelluloses [Figure 2(a)]. This confirms that the peak in this temperature range is due mainly to degradation of hemicelluloses. While the T_{on} of HR increased compared with WF, the peak temperature of cellulose decomposition ($T_{p,c}$) remained almost same as that of WF. This observation is consistent with the DTG results of jute fiber.[8] These changes may result from the removal of easily degradable hemicelluloses, which decompose before cellulose does. Removal of lignin caused a decrease in thermal stability. The T_{on} and $T_{p,c}$ decreased from 230 and 361°C to 218 and 336°C, respectively (Table II). This likely resulted from the loss of the lignin fraction, which is more thermally stable than cellulose and hemicellulose.[22] The lignin acts as

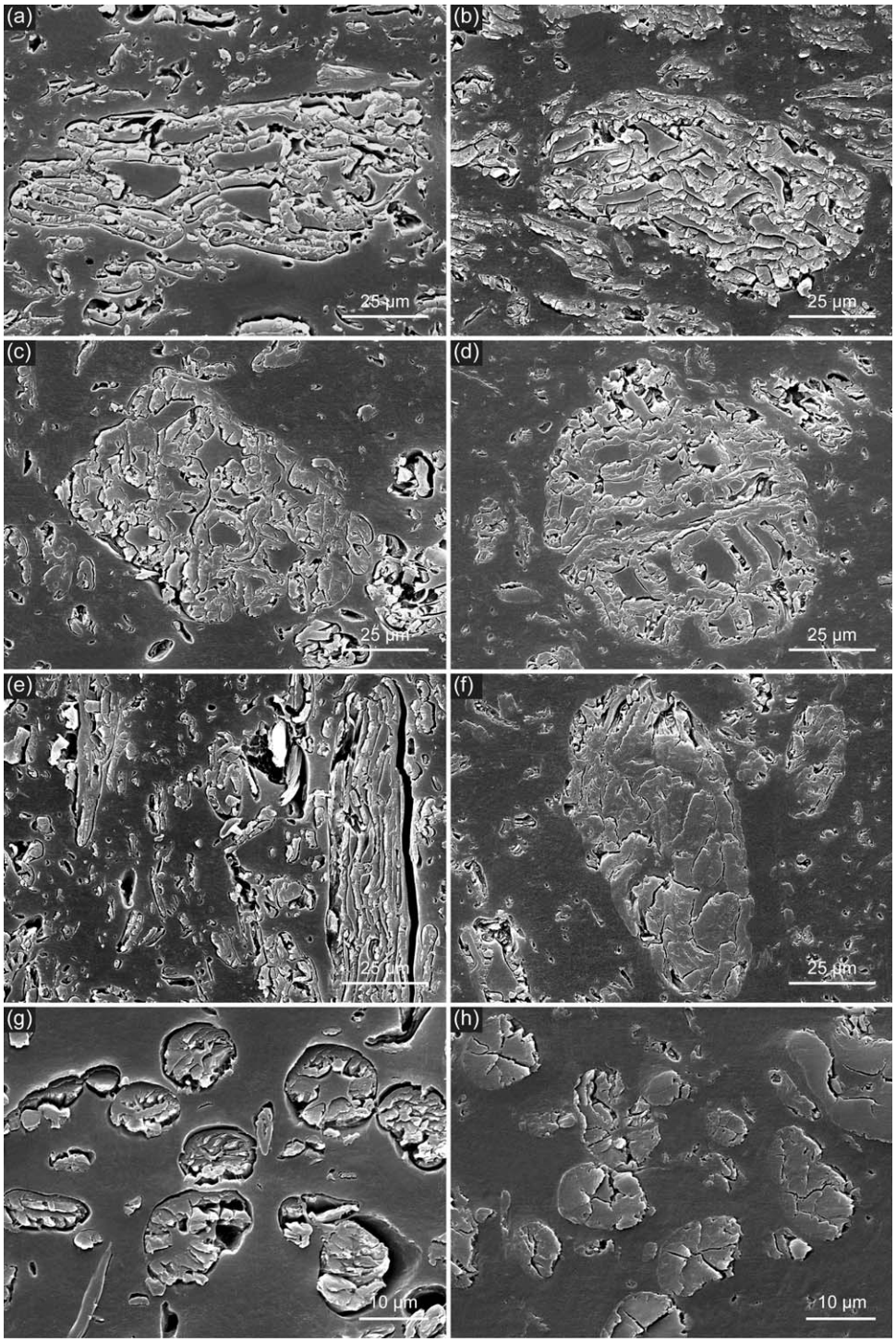

Figure 1. SEM micrographs of sectioned surface of the composites (a) WF/PE, (b) WF/PE/MA, (c) HR/PE, (d) HR/PE/MA, (e) HC/PE, (f) HC/PE/MA, (g) αC/PE, and (h) αC/PE/MA.

a protective barrier to heat via coating the cellulose.[23] Another possible explanation is that the molecular weight of cellulose decreased during delignification treatment,[24] which lowered the decomposition temperature. Removal of both hemicellulose and lignin caused an increase in T_{on} and a decrease in $T_{p,c}$. This resulted from the removal of the easily degradable hemicelluloses and the thermally stable lignin as, mentioned above.

The decomposition behavior of the WPs in composites exhibited the same trends as the individual WPs (Figure 2 and Table II). Compared with the degradation peak of neat HDPE, the $T_{p,h}$ of HDPE in the composites was shifted slightly to higher temperatures (Table II), irrespective of the particle type. This suggests an improvement in thermal stability of the HDPE matrix, due to incorporation of WPs.[25] The decomposition of

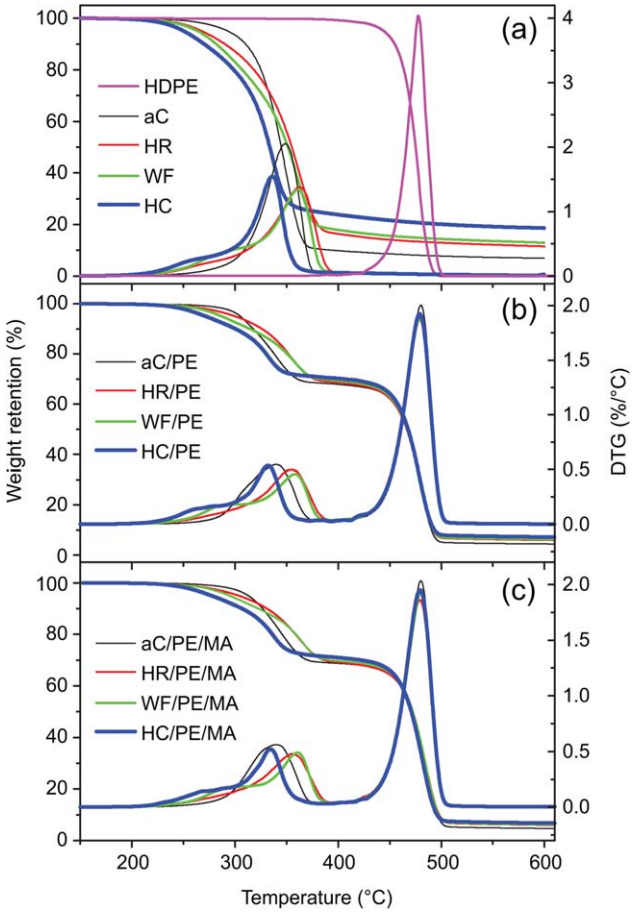

Figure 2. TGA and DTG curves of (a) neat HDPE and WPs, (b) composites without MAPE, and (c) with MAPE. [Color figure can be viewed in the online issue, which is available at wileyonlinelibrary.com.]

WPs began at temperatures below the T_{on} of HDPE. The char layer gradually accumulated to form a protective network, which can delay the decomposition process of the HDPE matrix that results from poor thermal conductivity of char.[25] The presence of HDPE matrix can protect WPs, thereby increasing the T_{on} of the composites, while the $T_{p,c}$ decreases compared with the individual WPs. A possible explanation could be that the molten HDPE matrix showed a higher thermal conductivity than that of WPs,[25] accelerating the decomposition of WPs. The T_{on} of MAPE coupled composites was slightly higher than that of the uncoupled ones. This behavior may be attributed to the enhanced interfacial adhesion between the matrix and the WPs. The incorporation of MAPE did not influence the $T_{p,c}$ and $T_{p,h}$.

DSC Analysis

The crystallization onset temperature (T_c) and crystallization peak temperature (T_p) of neat HDPE were 119.8 and 116.5°C, respectively (Table II). The T_c and T_p of the uncoupled and MAPE coupled composites shifted toward higher temperatures, ranging from 120.8 to 121.6°C and 117.9 to 119.5°C, respectively (Table II). This indicates that the crystallization starts at higher temperatures, arising possibly from the nucleating effect of WPs.[26] This phenomenon is, however, inconsistent with our previous conclusion that poplar wood sawdust does not act as a nucleating agent for the HDPE matrix.[27,28] This behavior indicates that the nucleation activity of WP is highly dependent on wood sources and topography.[28]

The slope in the higher temperature side of the cooling curve [Figure 3(a)], S_i, is a measure of the nucleation rate for crystallization; the higher the value, the faster the nucleation rate.[29] $T_c - T_p$ is a measure of the crystal growth rate; the lower the value, the higher the crystal growth rate.[29] Early crystallization is initiated for the composites, but the nucleation rate of crystallization decreased (decrease in S_i), especially for αC/PE and HR/PE (Table II). The value of S_i decreased from 7.20 to 2.77 and 4.70 for αC/PE and HE/PE, respectively. The value of $T_c - T_p$ increased from 2.4 to 3.3°C and 2.6°C for αC/PE and HR/PE, respectively, indicating a decrease in the crystal growth rate. A lower crystallization nucleation rate and growth rate results in a thicker crystal lattice[26] as indicated by the higher melting peak temperature (T_m) of the composites (Table II), especially for αC/PE and HR/PE. The α-Cellulose used in this study had the highest aspect ratio among the four particle types and its crystal form is cellulose II. The crystal form of HR was partially transformed from cellulose I to cellulose II (not shown). Chen and Yan[26] concluded that relatively long fibers have poor nucleating ability. Borysiak reported that the nucleating effect of wood fillers occurs only in the presence of cellulose I.[30] Transformation of cellulose I to cellulose II weakened the nucleating ability, while the fillers containing only cellulose II did not induce the transcrystallinity layer. The above factors lowered the crystallization nucleation rate and growth rate of αC/PE and HR/PE compared with the other uncoupled composites (Table II).

The incorporation of MAPE in the composites caused an increase in T_c and T_p, and a decrease in T_m, suggesting an improved nucleating ability of WPs after the addition of MAPE.[29] This in turn resulted in a higher degree of crystallinity (X_c) of the composites (Table II). The X_c of HR/PE, HC/PE, and αC/PE increased from 74.6, 73.8, and 69.9% to 78.2, 76.8, and 78.1% for HR/PE/MA, HC/PE/MA, and αC/PE/MA, respectively. This behavior may be associated with the high mobility of the MAPE molecular chains, which penetrated and grafted to the WP surface increasing the interfacial adhesion of wood with HDPE chains, enhancing nucleating ability.[31] However, this behavior did not occur in WF/PE/MA. The incorporation of MAPE into WF/PE obtained the opposite effect compared to the other composites (Table II). The X_c of WF/PE decreased from 72.6 to 69.8% for WF/PE/MA. The exact cause of this phenomenon cannot be predicted under the scope of this investigation.

Dynamic Rheological Analysis

The average diameter of αC, HR, HC, and WF before extrusion and injection molding is 34.2, 81.7, 81.9, 74.2 μm, respectively. In addition, the size of the fibers will be reduced after processing. At a wood content of 40%, changing the particle size (80–100, 100–160, and >160 mesh) of WF did not apparently influence the melt viscosity (data not shown). A comparable study by Li and Wolcott also showed that the various size of WP ranging from 80 to 140 mesh did not substantially change

Table II. The Results of TGA and DSC Analysis

Sample	T_{on}[a] (°C)	$T_{p,w}$[b] (°C)	$T_{p,h}$[c] (°C)	T_c[d] (°C)	T_p[e] (°C)	$T_c - T_p$[f] (°C)	S_i[g]	$T_{m,p}$[h] (°C)	X_c[i] (%)
WF	230.1 (0.5)	361.1 (0.4)	–	–	–	–	–	–	–
HR	232.9 (0.2)	362.6 (0.1)	–	–	–	–	–	–	–
HC	218.2 (0.3)	336.1 (0.2)	–	–	–	–	–	–	–
αC	253.0 (0.3)	348.7 (0.1)	–	–	–	–	–	–	–
HDPE	427.8 (0.0)	–	477.7 (0.0)	119.2 (0.0)	116.8 (0.0)	2.4	7.20 (0.2)	133.2 (0.2)	62.5 (0.8)
WF/PE	250.0 (0.4)	357.8 (0.3)	479.0 (0.0)	121.3 (0.0)	118.9 (0.0)	2.4	7.10 (0.1)	134.2 (0.5)	72.6 (0.4)
HR/PE	255.2 (0.3)	354.6 (1.4)	479.3 (0.0)	121.3 (0.0)	118.7 (0.0)	2.6	4.70 (0.1)	135.1 (0.1)	74.6 (1.8)
HC/PE	236.0 (0.2)	332.2 (0.1)	479.0 (0.3)	121.4 (0.0)	119.1 (0.1)	2.3	6.08 (0.1)	134.3 (0.2)	73.8 (1.2)
αC/PE	275.3 (0.2)	339.6 (0.1)	480.2 (0.2)	121.4 (0.1)	118.1 (0.5)	3.3	2.77 (0.2)	136.3 (0.6)	69.9 (1.7)
WF/PE/MA	252.9 (0.3)	360.7 (0.6)	480.2 (0.4)	120.8 (0.0)	117.9 (0.3)	2.9	1.72 (0.1)	134.7 (0.2)	69.8 (0.9)
HR/PE/MA	255.3 (0.2)	355.2 (0.2)	479.2 (0.1)	121.6 (0.1)	119.3 (0.1)	2.3	5.77 (0.2)	133.9 (0.4)	78.2 (0.4)
HC/PE/MA	239.1 (0.1)	334.4 (0.2)	479.4 (0.1)	121.5 (0.0)	119.2 (0.2)	2.3	5.46 (0.2)	133.7 (0.0)	76.8 (1.2)
αC/PE/MA	277.0 (0.8)	339.7 (1.2)	480.2 (0.5)	121.6 (0.1)	119.5 (0.0)	2.1	5.82 (0.1)	134.3 (0.0)	78.1 (0.8)

[a] Onset decomposition temperature (1% weight loss).
[b] Peak temperature of wood from DTG curve.
[c] Peak temperature of HDPE from DTG curve.
[d] Crystallization onset temperature.
[e] Crystallization peak temperature.
[f] Difference between crystallization onset and peak temperature.
[g] Slope in the higher temperature side of the cooling curve.
[h] Melting peak temperature.
[i] Degree of crystallinity calculated with the enthalpy of melting.

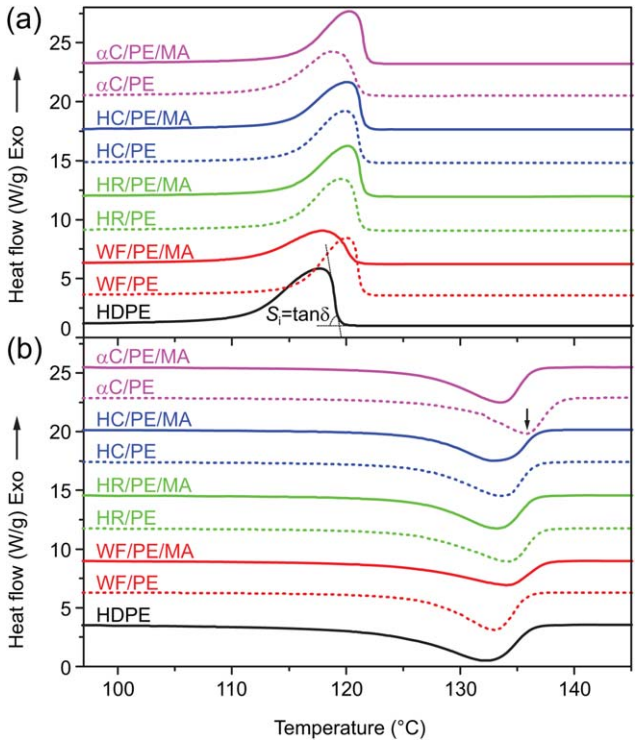

Figure 3. DSC cooling (a) and heating thermogram (b) of neat HDPE and the composites. [Color figure can be viewed in the online issue, which is available at wileyonlinelibrary.com.]

either the shear or the extensional viscosity of maple wood/HDPE (60/40 in weight) composites[2]. Accordingly, we assumed that the influence of particle size on the rheological properties of the four WPs (αC, HR, HC, and WF)/HDPE melts could be disregarded.

The removal of cell wall composition had a significant effect on the rheological behavior of the composite melt (Figure 4). Incorporation of HR and αC into the HDPE matrix weakened the dependence of storage modulus (G') and loss modulus (G'') on the frequency, as compared with the WF-based composite, especially at low frequencies [Figure 4(a,b)]. At low frequencies, the G' and G'' of αC/PE melt tend to reach a plateau that is attributed to the concentration of relaxation and the presence of apparent yield stress owing to interactions between the dispersed particles.[32] The αC that was used had the highest aspect ratio (7.54, 3.95, 3.67, and 3.32 for αC, HR, HC, and WF, respectively) and degree of crystallinity (72.0, 57.4, 51.1, and 43.5% for αC, HR, HC, and WF, respectively) among the four types of particles. The low-frequency plateau of αC/PE therefore may be attributed to the formation of an interconnected αC network in the HDPE matrix, which restrains the motion of HDPE chains. This resulted in a higher G' and G'' compared with the other composite melts.[33] HC/PE exhibited the highest tensile modulus and storage modulus (E') at room temperature (not shown), resulting from the highest level of deformation of HC. However, the HC/PE melt exhibited the lowest G' and G'' [Figure 4(a,b)]. This behavior resulted from the fact that the restrained deformation caused by HDPE disappeared in the molten state. The porous HC had a higher flexibility, resulting

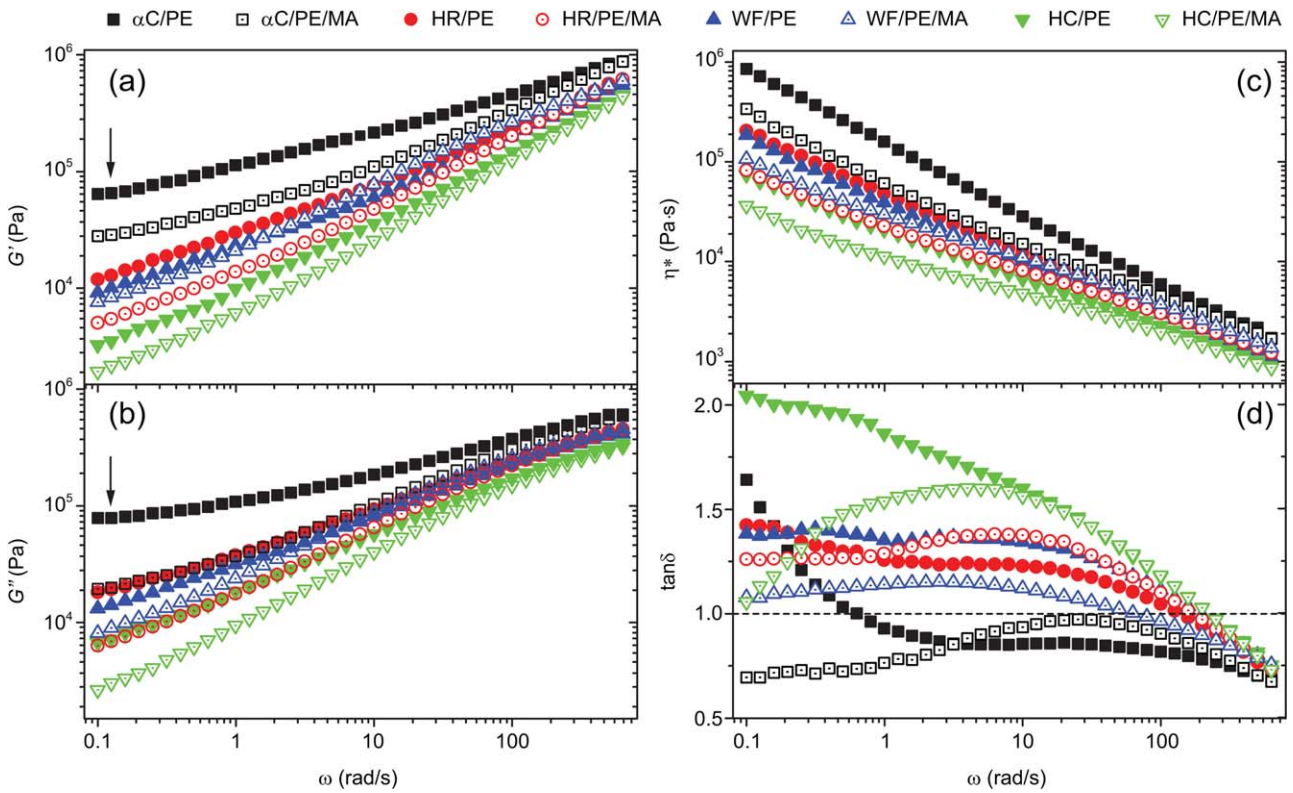

Figure 4. (a) Storage modulus (G'), (b) loss modulus (G''), (c) complex viscosity (η^*), and (d) tanδ of the composite melts. [Color figure can be viewed in the online issue, which is available at wileyonlinelibrary.com.]

in less hindrance to the mobility of HDPE molecular chains at higher temperatures. The G' and G'' of the HR/PE melt were slightly higher than those of WF/PE melt, possibly because the HR has a higher crystallinity and aspect ratio than WF, but much lower than those of the αC/PE melt.

Our results show that complex viscosity (η^*) of the composite melts decreased linearly with increasing angular frequency, regardless of particle type [Figure 4(c)]. The viscosity of the melt decreased in the following order: αC/PE > HR/PE > WF/PE > HC/PE. Although at low frequencies, the viscosity difference for the melts was pronounced, at higher frequencies the difference was reduced and the curves seemed to converge. This phenomenon is primarily attributed to the pseudoplastic shear thinning effect, which is more prominent for αC/PE, resulting from more intensive interaction between particles. Therefore, it requires higher shear stress and longer relaxation time to allow αC/PE to flow.[34] However, the significant decrease in viscosity at high frequencies implies that extrusion processing using particles with high aspect ratios may not be an issue if it runs at a high shear rate.

The improved interfacial adhesion resulting from the usage of coupling agents can limit the thermal motion of the matrix molecules, in turn increasing the modulus of the composite melts.[35] In this study, however, the incorporation of MAPE caused a considerable decrease in the storage modulus, loss modulus, and complex viscosity of the composite melts [Figure 4(a–c)]. This may be due to the decrease in interfacial tension and interparticle interaction from the improved particle dispersion. Furthermore, the MAPE acts as an internal lubricant in the composites because the MAPE had a lower molecular weight than HDPE matrix.[3] For composite melts with MAPE, removal of lignin and both hemicellulose and lignin showed the same influence on the storage modulus, loss modulus, and complex viscosity as the composite melt without MAPE, namely αC/PE/MA > WF/PE/MA > HC/PE/MA (Figure 4). However, removal of hemicellulose had the inverse influence: WF/PE/MA > HR/PE/MA. This may be due to removal of hemicellulose a decreasing the number of hydroxyl groups on the HR surface significantly, which can react with the maleic anhydride moieties of MAPE. An excess of MAPE without a reaction in the composites can act as an internal lubricant decreasing the melt viscosity and moduli.

At the low frequency region, the damping factor tan δ ($= G''/G'$) is >1.0 [Figure 4(d)], so that the loss modulus dominates the storage modulus. This indicates a viscous response, because at low frequency, there is sufficient time to allow polymer chains to relax.[36] The tan δ dropped sharply at higher frequencies by crossing the reference line of tan $\delta = 1$. The cross point (tan $\delta = 1$) of HC/PE was observed at 250.1 rad/s, and shifted toward lower frequencies of 198.7, 125.4, and 0.628 rad/s for WF/PE, HR/PE, and αC/PE, respectively. The tan δ amplitude above 0.2 rad/s decreased in the following order: HC/PE > WF/PE > HR/PE > αC/PE. High stiffness of the reinforcing particles may limit the mobility and deformation of the matrix molecules. As a result, the composites exhibited a great storage modulus, a small viscoelastic lag between the stress and strain, and a low tan δ.[34] Beyond the cross point, G'' became smaller than G' and showed

a plateau-like, nonterminal behavior, which indicating the elastic characteristic of the melts.[3] This behavior was due to the insufficient relax time at higher frequencies, which strengthens the elastic nature of the HDPE melt. The incorporation of MAPE had a different influence on the tan δ of the composites. At low frequencies, the tan δ of αC/PE/MA and HR/PE/MA was lower than that of αC/PE and HE/PE, respectively, while it was higher at high frequencies. The tan δ of αC/PE/MA was <1.0 through the frequency range. The tan δ of WF/PE/MA and HC/PE/MA was lower than that of WF/PE and HC/PE in the frequency range, respectively.

CONCLUSIONS

Based on the results of this study the following conclusions can be drawn:

1. Removal of hemicellulose improved the thermal stability of the composites; removal of lignin decreased the thermal stability of the composites; removal of both hemicellulose and lignin increased the thermal stability of the composites.
2. Removal of hemicellulose decreased the crystallization nucleation rate and growth rate of αC/PE and HR/PE compared to WF/PE.
3. Removal of lignin decreased the storage modulus, loss modulus, and complex viscosity of composite melts with and without MAPE due to the improved flexibility and deformability of HC. Removal of both hemicellulose and lignin resulted in highest melt moduli and viscosity of composite melts with and without MAPE.

This study found that enhancing the plasticity of rigid cell walls may be a useful strategy to improve the processability of WPCs. This study laid groundwork for future research on the role of cell wall modification in WPC processing. Our future researches will focus on the effect of removal of cell wall composition on the long-term durability of the composites during outdoor service.

ACKNOWLEDGMENTS

The supports from the National Key Technologies R&D Program of China (No. 2012BAD32B04) and National Natural Science Foundation of China (Nos. 31010103905, 31070507, and 31100425) are gratefully acknowledged. Yanjun Xie thanks the Program for New Century Excellent Talents in University of Ministry of Education of China (No. NCET-11-0608).

REFERENCES

1. Liu, H.; Wu, Q.; Han, G.; Yao, F.; Kojima, Y.; Suzuki, S. *Compos. A* **2008**, *39*, 1891.
2. Li, T. Q.; Wolcott, M. P. *Polym. Eng. Sci.* **2005**, *45*, 549.
3. Li, T. Q.; Wolcott, M. P. *Polym. Eng. Sci.* **2006**, *46*, 464.
4. Hristov, V.; Takacs, E.; Vlachopoulos, *J. Polym. Eng. Sci.* **2006**, *46*, 1204.
5. Wang, Q.; Ou, R.; Shen, X.; Xie, Y. *BioResources* **2011**, *6*, 3621.
6. Kumar, R.; Hu, F.; Hubbell, C. A.; Ragauskas, A. J.; Wyman, C. E. *Bioresource Technol.* **2013**, *130*, 372.
7. Koehler, L.; Telewski, F. W. *Am. J. Bot.* **2006**, *93*, 1433.
8. Roy, A.; Chakraborty, S.; Kundu, S. P.; Basak, R. K.; Basu Majumder, S.; Adhikari, B. *Bioresource Technol.* **2012**, *107*, 222.
9. Hosseinaei, O.; Wang, S.; Enayati, A. A.; Rials, T. G. *Compos. A* **2012**, *43*, 686.
10. Mukherjee, A.; Ganguly, P. K.; Sur, D. *J. Text. I.* **1993**, *84*, 348.
11. Fabiyi, J. S.; McDonald, A. G.; McIlroy, D. *J. Polym. Environ.* **2009**, *17*, 34.
12. Andrusyk, L.; Oporto, G. S.; Gardner, D. J.; Neivandt, D. J. Proceedings of the 51st Int. Conv. Soc. of Wood Sci. and Tech., Concepción, Chile, November, **2008**.
13. Hosseinaei, O.; Wang, S.; Taylor, A. M.; Kim, J. W. *Int. Biodeter. Biodegr.* **2012**, *71*, 29.
14. Pelaez-Samaniego Manuel, R.; Yadama, V.; Lowell, E.; Amidon Thomas, E.; Chaffee Timothy, L. *Holzforschung* **2013**, *67*, 193.
15. Karimi, A.; Nazari, S.; Ghasemi, I.; Tajvidi, M.; Ebrahimi, G. *J. Appl. Polym. Sci.* **2006**, *102*, 4759.
16. Fabiyi, J. S.; McDonald, A. G. *J. Reinf. Plast. Comp.* **2013**, *32*, 547.
17. Ou, R.; Xie, Y.; Wolcott, M. P.; Sui, S.; Wang, Q. Materials & Design Submitted.
18. TAPPI Test Method T 203 om-93. TAPPI Press, Atlanta, Georgia, USA, **1994**.
19. Wise, L. E.; Murphy, M.; D'Addieco, A. A. *Pap. Trade J.* **1964**, *122*, 35.
20. Bradrup, J.; Immergut, E. Polymer handbook; Wiley: New York, **1989**.
21. Ouajai, S.; Shanks, R. A. *Polym. Degrad. Stabil.* **2005**, *89*, 327.
22. Sarkar, S.; Adhikari, B. *J. Adhes. Sci. Technol.* **2000**, *14*, 1179.
23. Morandim-Giannetti, A. A.; Agnelli, J. A. M.; Lanças, B. Z.; Magnabosco, R.; Casarin, S. A.; Bettini, S. H. P. *Carbohydr. Polym.* **2012**, *87*, 2563.
24. Hubbell, C. A.; Ragauskas, A. *J. Bioresource Technol.* **2010**, *101*, 7410.
25. Zhao, Q.; Zhang, B.; Quan, H.; Yam, R. C. M.; Yuen, R. K. K.; Li, R. K. Y. *Compos. Sci. Technol.* **2009**, *69*, 2675.
26. Chen, J.; Yan, N. *Compos. B* **2013**, *54*, 180.
27. Ou, R.; Guo, C.; Xie, Y.; Wang, Q. *BioResources* **2011**, *6*, 4547.
28. Ou, R.; Xie, Y.; Guo, C.; Wang, Q. *J. Appl. Polym. Sci.* **2012**, *126*, E2.
29. Sewda, K.; Maiti, S. N. *J. Appl. Polym. Sci.* **2010**,*118*, 2264.
30. Borysiak, S. *J. Therm. Anal. Calorim.* **2013**, *113*, 281.
31. Hristov, V.; Vasileva, S. *Macromol. Mater. Eng.* **2003**, *288*, 798.
32. Bousmina, M.; Muller, R. *Rheol. Acta* **1996**, *35*, 369.
33. Aranguren, M. I.; Mora, E.; DeGroot, J. V.; Macoscko, C. W. *J. Rheol.* **1992**, *36*, 1165.
34. Lozano, K.; Yang, S. Y.; Zeng, Q. *J. Appl. Polym. Sci.* **2004**, *93*, 155.
35. Hristov, V.; Vlachopoulos, J. *Macromol. Mater. Eng.* **2007**, *292*, 608.
36. Nayak, S. K.; Mohanty, S.; Samal, S. K. *Mater. Sci. Eng. A* **2009**, *523*, 32.